

# Phylogenetic and Kinetic Characterization of a Suite of Dehydrogenases from a Newly Isolated Bacterium, Strain SG61-1L, That Catalyze the Turnover of Guaiacylglycerol- $\beta$ -Guaiacyl Ether Stereoisomers

Shannu Palamuru,<sup>a,b</sup> Nikki Dellas,<sup>a</sup> Stephen L. Pearce,<sup>a</sup> Andrew C. Warden,<sup>a</sup> John G. Oakeshott,<sup>a</sup> Gunjan Pandey<sup>a</sup>

CSIRO Land & Water Flagship, Acton, ACT, Australia<sup>a</sup>; Research School of Chemistry, Australian National University, Acton, ACT, Australia<sup>b</sup>

**Lignin is a complex aromatic polymer found in plant cell walls that makes up 15 to 40% of plant biomass. The degradation of lignin substructures by bacteria is of emerging interest because it could provide renewable alternative feedstocks and intermediates for chemical manufacturing industries. We have isolated a bacterium, strain SG61-1L, that rapidly degrades all of the stereoisomers of one lignin substructure, guaiacylglycerol- $\beta$ -guaiacyl ether (GGE), which contains a key  $\beta$ -O-4 linkage found in most intermonomer linkages in lignin. In an effort to understand the rapid degradation of GGE by this bacterium, we heterologously expressed and kinetically characterized a suite of dehydrogenase candidates for the first known step of GGE degradation. We identified a clade of active GGE dehydrogenases and also several other dehydrogenases outside this clade that were all able to oxidize GGE. Several candidates exhibited stereoselectivity toward the GGE stereoisomers, while others had higher levels of catalytic performance than previously described GGE dehydrogenases for all four stereoisomers, indicating a variety of potential applications for these enzymes in the manufacture of lignin-derived commodities.**

The lignin polymer, representing 15 to 40% of plant-derived biomass, is a potential renewable alternative to petrochemical feedstocks for chemical manufacturing industries, particularly with regard to aromatic compounds (1). One of the major hurdles for the utilization of lignin in this way is its recalcitrance; the polymeric structure of lignin coupled with the nature of its chemical bonds renders it highly resistant to chemical or biological degradation. Chemical degradation of lignin has been utilized by some industries, but it usually involves nonselective destruction of lignin via burning or treatment under highly alkaline conditions, which renders it less useful or of lower value to many downstream applications (2). The biological depolymerization of lignin should be a more selective and energy-efficient process and therefore potentially a cost-effective and environmentally sustainable alternative to the chemical processes currently employed (2). However, to date, the identification of suitable biocatalysts involved in lignin depolymerization has proven difficult.

Lignin has a polyaromatic structure with more than five different types of intermonomer linkages (3); the  $\beta$ -O-4 linkage (also known as the  $\beta$ -aryl ether linkage) represents 45 to 70% of these linkages (4, 5). The first step in the biological degradation of the lignin polymer occurs nonspecifically through the action of laccases and extracellular peroxidase enzymes (manganese peroxidase, versatile peroxidase, and lignin peroxidase) via radical ion mechanisms (5–7). While fungi are thought to be the main contributors to lignin degradation, recent reports on bacteria and their enzymes suggest that certain bacterial strains may also play a role in lignin polymer or kraft lignin degradation (8–23). While the early steps involved in the biological degradation of the lignin polymer are nonspecific, a few bacteria have shown potential in directly and specifically degrading smaller units of the lignin polymer into industrially useful chemicals (4, 24–31).

In the 1980s, bacterial dehydrogenases from *Pseudomonas* spp. were isolated and found to catalyze C- $\alpha$ -alcohol oxidation of

$\beta$ -aryl ether- or diarylpropane-linked lignin dimers (28, 32). In this case, the proteins responsible were not identified and the degradation pathways were not further explored. Subsequently, however, dehydrogenases catalyzing such reactions from another bacterium, *Sphingomonas paucimobilis* SYK-6, have been characterized. SYK-6 has been reported to degrade several different types of model lignin dimers (5), including a molecule with a  $\beta$ -O-4 linkage known as guaiacylglycerol- $\beta$ -guaiacyl ether (GGE). The proposed pathway for the degradation of GGE in this organism begins with the oxidation of GGE via one of several C- $\alpha$ -dehydrogenases (LigD, LigO, LigL, or LigN) (33), followed by ether bond cleavage via one of several glutathione S-transferases (GSTs; LigE, LigF, or LigP) (34, 35), and then glutathione removal via one of several GSTs (LigG and probably others that have yet to be identified) (34, 36) (Fig. 1A). These reactions generate the end

Received 19 May 2015 Accepted 15 September 2015

Accepted manuscript posted online 18 September 2015

Citation Palamuru S, Dellas N, Pearce SL, Warden AC, Oakeshott JG, Pandey G. 2015. Phylogenetic and kinetic characterization of a suite of dehydrogenases from a newly isolated bacterium, strain SG61-1L, that catalyze the turnover of guaiacylglycerol- $\beta$ -guaiacyl ether stereoisomers. *Appl Environ Microbiol* 81:8164–8176. doi:10.1128/AEM.01573-15.

Editor: R. E. Parales

Address correspondence to Gunjan Pandey, gunjan.pandey@csiro.au.

S.P. and N.D. contributed equally to this work.

Supplemental material for this article may be found at <http://dx.doi.org/10.1128/AEM.01573-15>.

Copyright © 2015, Palamuru et al. This is an open-access article distributed under the terms of the [Creative Commons Attribution-Noncommercial-ShareAlike 3.0 Unported license](https://creativecommons.org/licenses/by-nc-sa/4.0/), which permits unrestricted noncommercial use, distribution, and reproduction in any medium, provided the original author and source are credited.

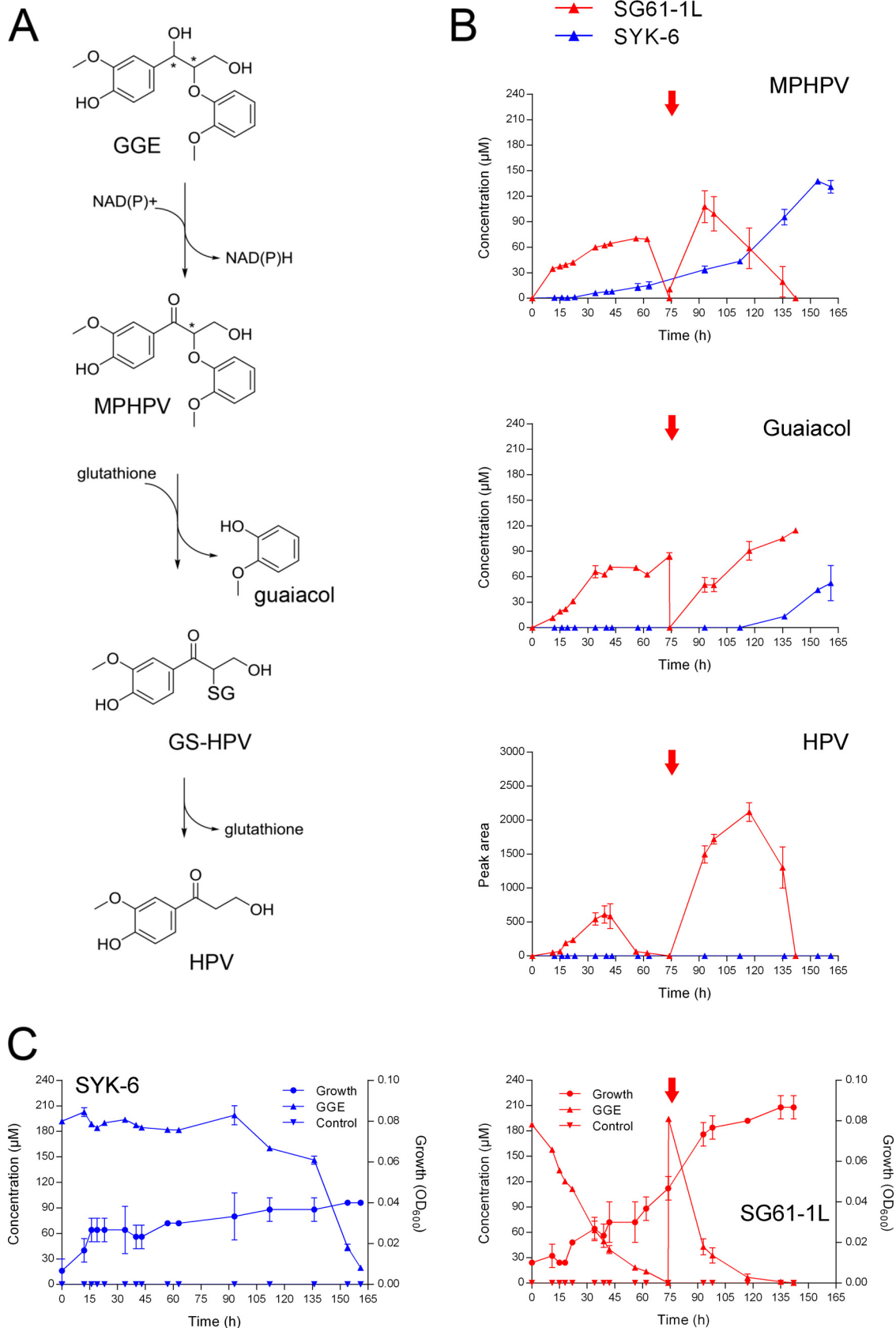


**FIG 1** Bacterial growth and degradation of GGE. (A) Pathway for the transformation of GGE to HPV in SYK-6 and SG61-1L. (B) Metabolite formation and disappearance over the course of the GGE growth cell experiment in SG61-1L (red) and SYK-6 (blue). Each graph depicts a different metabolite (labeled in the upper right corner). (C) GGE degradation (left y axis) and bacterial growth (right y axis) over time for SYK-6 (left) and SG61-1L (right) during growth cell experiments with GGE as the sole carbon source compared with control experiments with no carbon source. The arrows indicate the time at which cultures of SG61-1L were pelleted and resuspended in fresh MM supplemented with GGE as described in Materials and Methods.

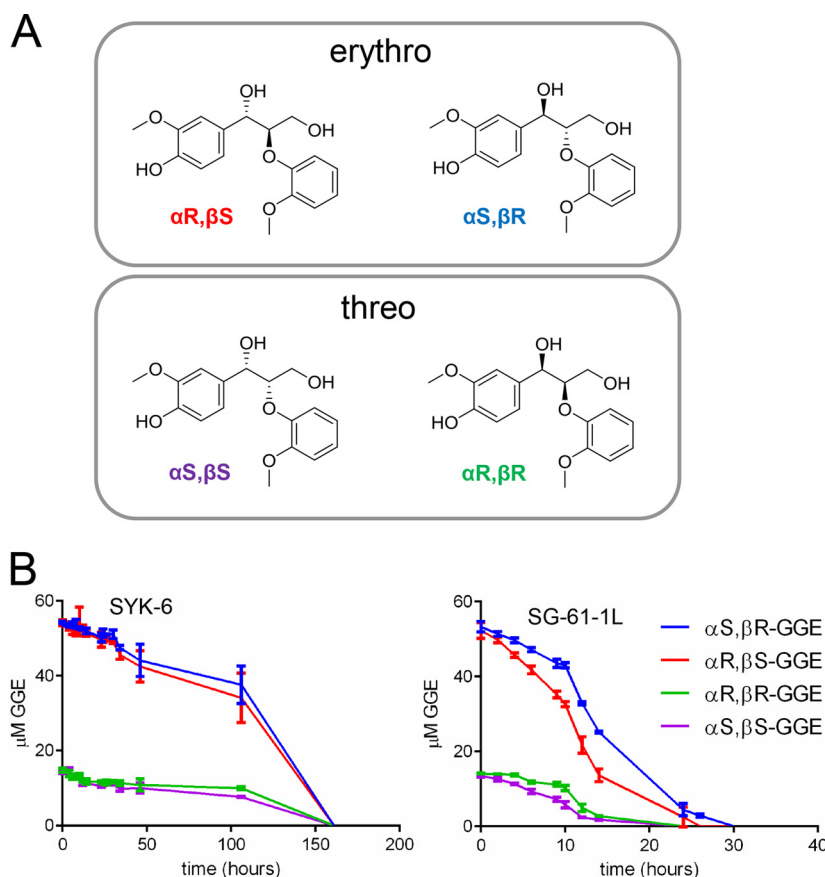


**FIG 2** GGE stereoisomer preferences during growth experiments. (A) The four GGE stereoisomers grouped according to enantiomer pairs (erythro and threo). (B) GGE stereoisomer degradation measured from growth cell experiments run on a chiral column (color coded by stereoisomer).

products guaiacol and  $\beta$ -hydroxypropiovanillone (HPV), the latter of which is eventually fed into the protocatechuate 4,5-cleavage pathway (4, 5). In SYK-6, the biological conversion of GGE to HPV and guaiacol is performed by a series of stereoselective enzymes (33, 36, 37); there are two stereocenters in the GGE molecule and therefore four possible stereoisomers (Fig. 2A). Expression of the C- $\alpha$ -dehydrogenases LigD, LigO, LigL, and LigN in *Escherichia coli* and gene disruption experiments with SYK-6 showed that these enzymes are responsible for the first step in the pathway, collectively oxidizing all of the GGE stereoisomers but individually exhibiting preference for one or two of them (33).

While bacteria are able to degrade intermonomer linkages of lignin substructures, their reported degradation rates are either not known or quite low (28, 31, 38, 39), and optimization of these transformation pathways (and the enzymes involved) is paramount for their industrial utilization. Here we report the isolation of a bacterium (SG61-1L) that is able to degrade a GGE model lignin dimer at a significantly higher rate than SYK-6. These results led to our identification of several enzyme candidates with robust activities for industrial transformation of a key intermediate in the biological breakdown of the lignin polymer.

## MATERIALS AND METHODS

**Materials.** (+)/(−)-GGE [1-(4-hydroxy-3-methoxyphenyl)-2-(2-methoxyphenoxy)propane-1,3-diol] was custom synthesized (>95% purity) by Albany Molecular Research Inc. (Albany, NY, USA). The percent com-

position of each stereoisomer in GGE was as follows: 39.5% ( $\alpha$ S, $\beta$ R)-GGE, 39.5% ( $\alpha$ R, $\beta$ S)-GGE, 10.5% ( $\alpha$ S, $\beta$ S)-GGE, and 10.5% ( $\alpha$ R, $\beta$ R)-GGE (see Fig. S1 in the supplemental material). The four individual stereoisomers ( $\alpha$ R, $\beta$ S)-, ( $\alpha$ S, $\beta$ R)-, ( $\alpha$ S, $\beta$ S)-, and ( $\alpha$ R, $\beta$ R)-GGE were a gift from Eiji Masai (at 100, 88.8, 96, and 93% purity, respectively) (40). Vanillin, vanillic acid, guaiacol, and all other analytical grade chemicals were purchased from Sigma-Aldrich (St. Louis, MO, USA) unless otherwise specified. *Sphingobium* sp. strain SYK-6 was purchased separately from the National Institute of Technology and Evaluation Biological Resource Center culture collection (Kisarazu, Chiba, Japan). *Pseudomonas putida* KT2440 was purchased from DSMZ (Braunschweig, Germany).

**Media and growth conditions.** Minimal medium (MM) was prepared by adding 1.36 g  $\text{KH}_2\text{PO}_4$ , 1.78 g  $\text{Na}_2\text{HPO}_4 \cdot 2\text{H}_2\text{O}$ , 0.50 g  $\text{MgSO}_4 \cdot 7\text{H}_2\text{O}$ , and 0.50 g  $\text{NH}_4\text{Cl}$  to 900 ml of double-distilled water. The pH was adjusted to 7.2 with a 1 M NaOH solution and 1 ml of a trace element solution [prepared as a 1:1,000 stock with 1 liter of distilled water containing 0.10 g  $\text{Al}(\text{OH})_3$ , 0.05 g  $\text{SnCl}_2 \cdot 2\text{H}_2\text{O}$ , 0.05 g KI, 0.05 g LiCl, 0.08 g  $\text{MgSO}_4$ , 0.05 g  $\text{H}_3\text{BO}_3$ , 0.10 g  $\text{ZnSO}_4 \cdot 7\text{H}_2\text{O}$ , 0.01 g  $\text{CoCl}_2$ , 0.01 g  $\text{NiSO}_4 \cdot 6\text{H}_2\text{O}$ , 0.05 g  $\text{BaCl}_2$ , and 0.05 g  $(\text{NH}_4)_6\text{Mo}_7\text{O}_{24} \cdot 4\text{H}_2\text{O}$ ] was added. The solution was filter sterilized with 0.22- $\mu\text{m}$  Fast Cap-60 filters (Pall Life Sciences, Port Washington, NY) and diluted to a final volume of 1 liter. The nutrient agar, nutrient broth (NB), and Luria broth (LB) used as rich media for bacterial growth were purchased from Becton, Dickinson and Company (Franklin Lakes, NJ, USA).

**Instrumentation and analytical methods.** Samples from growth and resting-cell experiments were analyzed with an Agilent 1200 Infinity Series time of flight (TOF) liquid chromatography-mass spectrometry (LC-MS) instrument (Agilent Technologies, Santa Clara, CA). Metabolites

analyzed by TOF LC-MS were quantified with a diode array detector (DAD) over an extracted wavelength range of 275 to 280 nm with the Applied Biosystems Analyst QS 1.1 software package (Life Technologies, Carlsbad, CA). Standard curves were constructed for GGE, guaiacol, vanillin, and vanillic acid, and the identities of these metabolites throughout growth and resting-cell experiments were confirmed by comparison to the retention time in LC and TOF MS spectral data (see Table S1 in the supplemental material). A standard curve for  $\alpha$ -(2-methoxyphenoxy)- $\beta$ -HPV (MPHPV) was constructed following its biosynthesis from GGE as detailed in the supplemental material. The identity of HPV (for which a standard was not available) was assigned on the basis of TOF MS spectral data reported previously for the SYK-6 bacterium (41). Runs were performed with either a Grace Alltima C<sub>18</sub> column (4.6 by 250 mm; W. R. Grace & Co, Columbia, MD) or a CHIRALPAK IE chiral column (4.6 by 250 mm; Daicel Corporation, Tokyo, Japan). An isocratic method was developed for use with the C<sub>18</sub> column with a mobile phase of acetonitrile-water-formic acid (55:45:0.1) at a flow rate of 0.8 ml min<sup>-1</sup> for 15 min. All substrates and intermediates were monitored at 275 to 280 nm and quantified by peak area. A separate isocratic method was developed for use with the chiral column, involving a mobile phase of water-acetonitrile-ethyl acetate (85:15:2) containing 0.1% formic acid at a flow rate of 0.8 ml min<sup>-1</sup> for 35 min. All stereoisomers were quantified by peak area from DAD detection over an extracted wavelength range of 265 to 300 nm with the Agilent TOF software (version A.01.00; Agilent Technologies).

**Isolation of GGE-degrading bacteria.** Bacteria were isolated from environmental samples that were provided by the Australian Paper Maryvale Mill (Victoria, Australia). The samples were collected from several sewage sludge waste sites and from the membrane bioreactor at the paper mill. In the first round of enrichments, 1 g of the combined samples was inoculated into 100 ml of MM containing 157.5  $\mu$ M GGE as the sole carbon source. Enrichments were incubated in 500-ml baffled flasks at 28°C on a shaker at 200 rpm and monitored for loss of substrate every 24 h by TOF LC-MS with the Grace Alltima C<sub>18</sub> column by the isocratic method as described above. Once the substrate was reduced to <63  $\mu$ M, 1 ml of the culture was transferred to the next generation of enrichments and the process described above was repeated 11 times. Finally, the enrichments were plated onto quarter-strength NB agar plates and incubated at 28°C. After 1 week, morphologically different bacteria were isolated and individually tested for GGE-degrading activity by TOF LC-MS. The GGE-degrading bacteria were identified from their full-length 16S rRNA sequences, which were obtained by genome sequencing (described below). The most promising bacterial degrader of GGE isolated from these experiments was an alphaproteobacterium named SG61-1L.

**Dye decolorization experiments.** Isolated bacteria were streaked onto NB agar plates containing either Azure B (Sigma-Aldrich) or Reactive Black 5 (Sigma-Aldrich) at a final concentration of 0.4 mM. To prepare the plates, an aqueous dye solution was sterile filtered and then added to autoclaved quarter-strength NB agar. Plates were incubated at 28°C and observed for clearing of the dye accompanied by bacterial growth.

**Growth and resting-cell experiments.** SG61-1L and SYK-6 were grown in NB medium at 28°C and harvested at mid-log phase (at an optical density at 600 nm [OD<sub>600</sub>] of 0.7) by centrifugation at 4,648  $\times$  g for 15 min at 20°C. The cells were washed twice with MM and resuspended (to a final OD<sub>600</sub> of 0.7) in MM or 20 mM phosphate buffer (pH 7.2) for growth and resting-cell experiments, respectively. In the first set of growth culture experiments, washed cells were inoculated at 1%, wt/vol, into MM (pH 7.2) containing either 200  $\mu$ M GGE or 330  $\mu$ M vanillin as the sole carbon source and shaken at 200 rpm at 28°C. In GGE growth experiments, SG61-1L cells were pelleted following the disappearance of GGE and resuspended in the same volume of fresh MM supplemented with 200  $\mu$ M GGE, and both degradation and growth were again monitored over time at 28°C. Samples were collected at various time points, filtered, and analyzed by TOF LC-MS with the Grace Alltima C<sub>18</sub> column.

To determine the relative rates of bacterial degradation of each GGE stereoisomer, a second set of growth culture experiments was carried out

with MM supplemented with 157.5  $\mu$ M GGE as described above. The relative level of each stereoisomer present in the culture was monitored over time and analyzed via chiral separation of the four different GGE stereoisomers with the chiral column as described above. The four stereoisomers were identified on the basis of the correlation with elution profiles and mass spectral data from authentic standards (40). As a negative control, a third bacterium, *P. putida* KT2440 was separately tested in cell growth experiments with GGE as the sole carbon source according to the protocol described above.

In resting-cell experiments, a 35-ml volume of cells was grown at 28°C and cells were harvested at log phase (OD<sub>600</sub> values were 0.63 and 0.67 for SG61-1L and SYK-6, respectively), washed twice with phosphate buffer, and resuspended in 100 ml MM containing 157.5  $\mu$ M GGE as the only carbon source. Samples were collected and analyzed by TOF LC-MS with the C<sub>18</sub> column as described for the growth culture experiments. All experiments were performed in triplicate.

**Genome sequencing and nucleotide sequences.** Genomic DNA was isolated from a pure culture of SG61-1L with Qiagen Genomic DNA buffers and 500/G genomic tips (Qiagen, Hilden, Germany). Short (500-bp)- and long (2,000-bp)-insert libraries were sequenced by MiSeq Illumina technology at the Micromon DNA sequencing facility (Monash University, Melbourne, Australia). The raw reads were then assembled with the SPAdes assembler version 3.5.0 (42), which performs error correction, assembly, scaffolding, and mismatch correction. The final assembly was 3,771,711 bp long with a GC content of 63% and was composed of three scaffolds 3.6 Mb, 94 kb, and 10 kb in length. Annotation of this assembly was performed by the NCBI Prokaryotic Genome Annotation Pipeline and identified 3,209 protein-coding sequences, 49 tRNA sequences, and two rRNA clusters.

**Cloning and overexpression of dehydrogenase genes.** Thirteen candidate dehydrogenase genes were selected from SG61-1L on the basis of two sets of criteria: (i) percent amino acid identity to the four SYK-6 dehydrogenases and (ii) genomic context, i.e., proximity to genes that have the potential to function elsewhere in the GGE degradation pathway (Table 1). Eleven of the 13 candidates from SG61-1L (Table 1), in addition to the 4 genes originally characterized from SYK-6 (those for LigD, LigO, LigL, and LigN) (33), were PCR amplified with Phusion High-Fidelity DNA polymerase (New England BioLabs, Ipswich, MA) and Gateway primers containing *attB* sites and an N-terminal six-histidine tag (Table 2). *attB*-flanked PCR products were subcloned into the pDNR201 vector (Life Technologies) with BP Clonase II (Life Technologies) and subsequently cloned into the pDEST14 destination vector (Life Technologies) with LR Clonase II according to the manufacturer's protocol (Life Technologies). The remaining two gene candidates from SG61-1L, those for 724 and 3329, were PCR amplified (the primer sequences used are in Table 2) and subsequently cloned into pETcc2, a pET14b-derived vector (Novagen, Madison, WI) containing an N-terminal six-histidine tag and a thrombin cleavage site. All 17 expression plasmids were subsequently transformed into *E. coli* BL21(DE3)/pLysS cells (Life Technologies). One colony of each was inoculated into LB medium and grown overnight at 37°C. This culture was then transferred into a 1-liter culture of LB medium and grown at 37°C to an OD<sub>600</sub> of 0.8 to 1.0, at which point 0.5 mM isopropyl- $\beta$ -D-thiogalactopyranoside was added for induction. The culture was then transferred to 28°C and shaken overnight. Induced cultures were harvested by centrifugation at 6,000  $\times$  g for 20 min at 4°C.

**Protein purification.** The harvested pellet from each induced culture was resuspended in lysis buffer (10% glycerol, 50 mM Tris [pH 8], 100 mM NaCl, 20 mM imidazole) and disrupted at 15,000 lb/in<sup>2</sup> on a Microfluidics M-110P homogenizer (Microfluidics, Westwood, MA) at 4°C. The lysate was then centrifuged at 18,000  $\times$  g for 30 min at 4°C. The supernatant was applied to a gravity column containing nickel-nitrilotriacetic acid resin (Qiagen), washed with lysis buffer, and eluted in elution buffer (10% glycerol, 50 mM Tris [pH 8], 100 mM NaCl, 250 mM imidazole). The protein samples were dialyzed overnight at 4°C in dialysis buffer (50 mM Tris [pH 8], 100 mM NaCl), and protein concentrations were

**TABLE 1** Criteria for selection of GGE dehydrogenase candidates in SG-61-1L

Gene product	Locus tag	% identity to SYK-6 GGE dehydrogenases <sup>a</sup>	Genomic context
474	SZ64_16365	15–20 (LigD)	Immediately downstream of two 2,4'-dihydroxyacetophenone dioxygenase genes and upstream of one benzyl alcohol dehydrogenase gene
3726	SZ64_14315	16–20 (LigO)	3.2 kb upstream of 3730
3191	SZ64_15940	18–21 (LigN)	3.2 kb upstream of vanillate demethylase oxygenase gene (on opposite strand)
3730	SZ64_14335	17–22 (LigL)	3.2 kb downstream of 3726
3344	SZ64_12435	17–22 (LigO)	Downstream of two GST genes (6 kb) and upstream of an alcohol dehydrogenase gene (1 kb) and <i>ligM</i> (5 kb) <sup>b</sup>
3175	SZ64_16025	19–22 (LigL)	2.6 kb downstream of vanillate demethylase oxygenase gene
3329	SZ64_12360	28–31 (LigO)	3.5 kb downstream of genes in the protocatechuate 4,5-cleavage pathway
2549	SZ64_00035	27–34 (LigO)	Immediately downstream of 2550
2706	SZ64_01650	30–37 (LigL)	Immediately downstream of 2705
724	SZ64_15290	30–39 (LigO)	None
2705	SZ64_01645	34–42 (LigN)	Immediately upstream of 2706
2550	SZ64_00030	30–47 (LigL)	Immediately upstream of 2549
1498	SZ64_05225	30–67 (LigN)	1.1 kb downstream of an aldehyde dehydrogenase gene

<sup>a</sup> Percent amino acid identities to all four SYK-6 dehydrogenases (LigD, LigO, LigL, LigN) are written as ranges. The SYK-6 dehydrogenase with the highest percent amino acid identity to the candidate dehydrogenase is in parentheses.

<sup>b</sup> LigM, tetrahydrofolate-dependent O-demethylase, is an enzyme responsible for degradation of vanillate and syringate in SYK-6 (54).

measured with a NanoDrop ND-1000 UV-Vis spectrophotometer (Thermo Scientific, Waltham, MA); NanoDrop values were corrected on the basis of theoretical extinction coefficients. For the results of SDS-PAGE analysis of all of the purified proteins, see Fig. S4 in the supplemental material.

**Enzymatic transformation of GGE to MPHPV.** LC-MS monitoring of enzymatic transformation from GGE to MPHPV was performed under the following reaction conditions: 50  $\mu$ M purified enzyme SG61-1L 724, 20 mM Tris (pH 7.5), 5 mM NAD<sup>+</sup>, and 100  $\mu$ M GGE in a final volume of 100  $\mu$ l. The reaction mixture was incubated at 28°C for 12 h and quenched by the addition of acetonitrile prior to LC-MS analysis. LC-MS was performed as described above with the Grace Alltima C<sub>18</sub> column.

**Enzyme kinetics.** All enzymes were assayed against each of the four GGE stereoisomers on a SpectraMax M3 plate reader (Molecular Devices, Sunnyvale, CA). Reactions were performed at 28°C in a final volume of 50  $\mu$ l containing 2 mM NAD<sup>+</sup> or NADP<sup>+</sup>, 20 mM Tris (pH 7.5), and concentrations of substrate ranging from 0.1  $\mu$ M to 2 mM. The concentration of each enzyme was optimized for each reaction and ranged from 0.013 to 4.5  $\mu$ M. All reactions were set up in a 384-well plate and monitored by the increase in absorbance at 340 nm over time, consistent with reduction of the cofactor NAD(P)<sup>+</sup> to NAD(P)H. Initial velocities at each substrate concentration were corrected on the basis of standard curves constructed for the two products, MPHPV and NADH (see the supplemental material). All kinetic parameters were calculated with GraphPad Prism (GraphPad Software, La Jolla, CA, USA).

**Phylogenetic analysis.** A phylogenetic tree was constructed from an alignment of dehydrogenase protein sequences from SYK-6, SG61-1L, one closely related bacterium that was unable to transform GGE (*P. putida* KT2440; data not shown), and two other bacteria (*Novosphingobium aromaticivorans* DSM12444 and *Sphingobium chlorophenolicum* L-1) that may have the potential to degrade GGE on the basis of NCBI-nr blastp hits to GGE dehydrogenases from SYK-6. Deduced amino acid dehydrogenase sequences present in these five genomes that shared  $\geq$ 20% identity with any of the four previously characterized SYK-6 enzymes (LigD, LigO, LigL, LigN) or the seven most closely related enzymes from SG61-1L (named 724, 2550, 2549, 2705, 2706, 1498, and 3329) were included in the alignment. Also in the alignment were several functionally verified dehydrogenases from various organisms that were included on the basis of the same criteria for percent identity as described above (see Table S2 in the supplemental material). The alignment was constructed with MAFFT by using the L-

INS-i algorithm (43) and consisted of a total of 166 sequences (see Fig. S3 in the supplemental material). The program AliStat was used to remove poorly aligned positions within the alignment with a mask value of 98 (55). SymTest using Bowker's matched-pair test for symmetry was used to confirm that the amino acid sequences evolved under stationary, reversible, and homogeneous conditions (55). A maximum-likelihood phylogenetic tree was then constructed with the IQ-TREE server by an ultrafast bootstrap approximation approach with 10,000 replicates (44, 45).

**Nucleotide sequence accession numbers.** This whole-genome shotgun project has been deposited at DDBJ/EMBL/GenBank under accession no. JXQC00000000. The version used in this paper is the first version, JXQC01000000.

## RESULTS

**Isolation of a novel GGE-degrading bacterium.** GGE-degrading bacteria from a paper mill waste site were identified through a series of enrichments as described in Materials and Methods. After 12 generations of enrichment, cultures were plated and individual colonies were isolated and tested for the ability to degrade GGE. Of the 55 bacterial colonies tested, only 2 were able to degrade GGE as a sole carbon source. One of these strains degraded GGE at a very low rate; after 800 h, 7% of the GGE remained in the growth cultures (data not shown). The other strain, named SG61-1L, was pursued further because of its ability to completely degrade 200  $\mu$ M GGE in 75 h (Fig. 1C). The sequences of two identical full-length copies of 16S rRNA genes (1,481 bp) identified from the assembled genome (locus tags SZ64\_16285 and SZ64\_16315) of SG61-1L revealed that this alphaproteobacterium belongs to the family *Erythrobacteraceae*, in the same order as lignin-degrading *Sphingobium* sp. strain SYK-6 (*Sphingomonadales*). The full-length 16S rRNA genes from SG61-1L and SYK-6 are 94% identical. The 16S rRNA genes of SG61-1L are also 97 to 98% identical to those of several type strains, including *Altererythrobacter troitsensis* KMM 6042<sup>T</sup>, *Croceicoccus marinus* E4A9<sup>T</sup>, *Altererythrobacter dongtanensis* JM27<sup>T</sup>, *Altererythrobacter epoxidivorans* JCS350<sup>T</sup>, and *Altererythrobacter xinjiangensis* S3-63<sup>T</sup>.

**Dye decolorization screening.** Dye decolorization is widely used as a preliminary screen for the identification of microbes

TABLE 2 Primers used to clone SYK-6 and SG61-1L dehydrogenase genes

Primer	Sequence (5'-3')
SG61_474_N6×H_for	CCATGCATCACCATCACCATCACATGAAGACACTCGACCAGTTCGACATTC
SG61_474_N6×H_rev	CAC TTTGTACAAGAAAGCTGGGTCTAATCGTTGAGCGGCTTGATCGG
SG61-724_xho1_rev	TATTCTCGAGTCACTGCATGCATCGGGC
SG61-724_ndel_for	ATTACATATGAAGGATTTTGC GGGCCGC
SG61_1498_N6×H_for	CCATGCATCACCATCACCATCACATGAAGGAAGTTTCGCGGGAAGACCGCATTC
SG61_1498_N6×H_rev	CAC TTTGTACAAGAAAGCTGGGTCTAGTCGAGCGGCGGCCGTC
SG61_2549_N6×H_for	CCATGCATCACCATCACCATCACATGCAGGAACTGACAGGCAAGGTG
SG61_2549_N6×H_rev	CAC TTTGTACAAGAAAGCTGGGTCTAGTTCGCTCGCTGGAGCTGAATTC
SG61_2550_N6×H_for	CCATGCATCACCATCACCATCACATGCCATCGGAAGTTTCGAAGGAAAAG
SG61_2550_N6×H_rev	CAC TTTGTACAAGAAAGCTGGGTCTAATCGCCTTCTCCCGGTAGTTGC
SG61_2705_N6×H_for	CCATGCATCACCATCACCATCACATGCAGGACGTAGCCGAAAAGGCG
SG61_2705_N6×H_rev	CAC TTTGTACAAGAAAGCTGGGTCTAGGGTGCCTCGCATAGATGGGGCTG
SG61_2706_N6×H_for	CCATGCATCACCATCACCATCACATGCGTGAGTTTCGCGGCAAGACG
SG61_2706_N6×H_rev	CAC TTTGTACAAGAAAGCTGGGTCTAGCCCGCTGGCCAGAG
SG61_3175_N6×H_for	CCATGCATCACCATCACCATCACATGGATCCGGCAGGCAAGATCGCCATTG
SG61_3175_N6×H_rev	CAC TTTGTACAAGAAAGCTGGGTCTAGCCGCTAGCCGGCCATTTGGTG
SG61_3191_N6×H_for	CCATGCATCACCATCACCATCACATGCGTTTCAAGGACAAGGTCGTCCTCGTG
SG61_3191_N6×H_rev	CAC TTTGTACAAGAAAGCTGGGTCTAGCGCAGTCCAGCATGCCG
SG61-3329_ndel_for	ATTACATATGAGCACTGCTGATCGGCCCTGG
SG61-3329_bamHI_rev	TATTGGATCCTCAGGTCAAGTTCGTAAGGCTGATGACCAG
SG61_3344_N6×H_for	CCATGCATCACCATCACCATCACATGCAC TTTCAAGGGAATGCACATCGTC
SG61_3344_N6×H_rev	CAC TTTGTACAAGAAAGCTGGGTCTAGACCTCGATGCTCTCCAGCAC
SG61_3726_N6×H_for	CCATGCATCACCATCACCATCACATGAAGTTTCGAGGCCGTCATCC
SG61_3726_N6×H_rev	CAC TTTGTACAAGAAAGCTGGGTCTACCCCGCCGCGATGATGCCG
SG61_3730_N6×H_for	CCATGCATCACCATCACCATCACATGACCAAGCGCCACGAAGGCAAG
SG61_3730_N6×H_rev	CAC TTTGTACAAGAAAGCTGGGTCTAGATGTCGTTGCGGATCGTCGCCAG
ligO-syk6_N6×H_for	CCATGCATCACCATCACCATCACATGCAGGATCTGGAAGGGAAAAGTC
ligO-syk6_N6×H_rev	CAC TTTGTACAAGAAAGCTGGGTCTAATCGCTACCCGGCATGTCC
ligN-syk6_N6×H_for	CCATGCATCACCATCACCATCACATGTTGGACGTAAGCGGCAAGACCGCCTTC
ligN-syk6_N6×H_rev	CAC TTTGTACAAGAAAGCTGGGTCTAGAGCGGCTCGTCGAGCGGCTG
ligD-syk6_N6×H_for	CCATGCATCACCATCACCATCACATGAAGGATTTCCAGGATCAGGTCGCGTTC
ligD-syk6_N6×H_rev	CAC TTTGTACAAGAAAGCTGGGTCTAGGCGCCTTCTTGTGCGCCCTC
ligL-syk6_N6×H_for	CCATGCATCACCATCACCATCACATGGACATCGCAGGGACCAC
ligL-syk6_N6×H_rev	CAC TTTGTACAAGAAAGCTGGGTCTAGGCCTTCTCCTTCGGCAC
ligO-syk6_N6×H_for	CCATGCATCACCATCACCATCACATGCAGGATCTGGAAGGGAAAAGTC
ligO-syk6_N6×H_rev	CAC TTTGTACAAGAAAGCTGGGTCTAATCGCTACCCGGCATGTCC
ligN-syk6_N6×H_for	CCATGCATCACCATCACCATCACATGTTGGACGTAAGCGGCAAGACCGCCTTC
ligN-syk6_N6×H_rev	CAC TTTGTACAAGAAAGCTGGGTCTAGAGCGGCTCGTCGAGCGGCTG

and/or enzymes that can degrade lignin via radical ion mechanisms (9, 11, 46–48). The 55 bacteria isolated in this work, along with SYK-6, were tested for the ability to decolorize two dyes, Azure B and Reactive Black 5. Fourteen of these bacteria could decolorize Azure B, while two others could decolorize Reactive Black 5 (data not shown). Neither of the two GGE-degrading bacteria (SG61-1L and SYK-6) could decolorize either of the two dyes. These results indicate that dye screening may not necessarily be a reliable method for identifying bacteria that are able to degrade certain lignin substructures, especially those employing degradation routes that do not generate radical ions.

**Comparison of the GGE degradation rates of SG61-1L and SYK-6.** The growth and GGE degradation rates of SG61-1L and SYK-6 were measured by growing the cells in MM supplemented with the GGE stereoisomer mixture as the sole carbon source. Both SG61-1L and SYK-6 showed an increase in OD<sub>600</sub> and a progressive loss of GGE over time (Fig. 1C), but SG61-1L grew on GGE much faster than SYK-6 (Fig. 1). At 74 h, when the GGE was completely degraded by SG61-1L, the cells (OD<sub>600</sub> of 0.05) were removed by centrifugation and resuspended in a fresh lot of GGE

containing MM. The second lot of GGE was completely degraded in the next 60 h while the OD<sub>600</sub> of the culture rose to 0.09. The negative controls with no added carbon showed no detectable growth of either bacterium (Fig. 1C). Bacterial growth under conditions where vanillin (a catabolic intermediate of GGE in both strains) was used as the sole carbon source were comparable (per mole of carbon) to those observed for growth on GGE as the sole carbon source (Fig. S2 in the supplemental material), indicating that bacterial growth rates with GGE were real and not an artifact of growth from cellular reserves. With the exception of HPV (which did not appear in SYK-6 growth cultures over the measurement time period), the same metabolites were identified in both bacteria and correlated well with the mass spectral data, which were also consistent with previously published spectra for the metabolites produced by SYK-6 (41) (see Table S1 in the supplemental material).

Consistent with their respective growth and GGE degradation rates, the metabolites also appeared earlier in the SG61-1L culture supernatant than in the SYK-6 culture supernatant. Complete transformation of GGE to its oxidized product, MHPHV, oc-

curred within 75 h in SG61-1L but required over 160 h in SYK-6 (Fig. 1C). MPPHV did not build up in the SG61-1L growth culture supernatant and was continuously transformed to downstream metabolites, consistent with the appearance of guaiacol (a product of the MPPHV etherase reaction) after only a few hours of growth (Fig. 1). In contrast, MPPHV accumulated in the SYK-6 growth culture supernatant to levels well above that observed with SG61-1L and detectable levels of guaiacol did not appear until approximately 135 h (Fig. 1B).

A second set of growth experiments was then carried out with both bacteria and the same GGE mixture, but this time it was analyzed on the chiral column to determine the rates at which individual stereoisomers were degraded in the presence of a mixture of GGE stereoisomers (Fig. 2). Consistent with the first set of experiments discussed above, these experiments also demonstrated that the GGE substrate disappears more slowly in SYK-6 than in SG61-1L (Fig. 2B) (the absolute rates of GGE disappearance analyzed via the chiral column were performed separately and found to be slightly different from the rates obtained in the first set of growth experiments, for reasons that could not be determined). Both bacteria degraded the pair of erythro enantiomers [( $\alpha$ R, $\beta$ S)-GGE and ( $\alpha$ S, $\beta$ R)-GGE] at an overall higher rate than the threo enantiomers [( $\alpha$ R, $\beta$ R)-GGE and ( $\alpha$ S, $\beta$ S)-GGE] (Fig. 2). However, the rates of the two members of each enantiomer pair differed in SG61-1L but could not be distinguished in SYK-6. In SG61-1L, the erythro isomer ( $\alpha$ R, $\beta$ S)-GGE disappeared slightly earlier than its enantiomer, ( $\alpha$ S, $\beta$ R)-GGE, and the threo isomer ( $\alpha$ S, $\beta$ S)-GGE also disappeared slightly earlier than its enantiomer, ( $\alpha$ R, $\beta$ R)-GGE (Fig. 2). The relative stereoisomer concentrations in the mixture were calculated by TOF LC-MS with a chiral column through the quantification of peak areas by using standard curves generated with authentic standards of all four stereoisomers.

Resting-cell experiments were performed in order to more rigorously decipher differences in degradation rates independent of cell growth for the two bacteria. The same metabolites appeared in these studies, which further validates that the same functional catabolic pathway is operating in both strains (data not shown). Because of limited cell growth, metabolites derived from HPV degradation (not observed during growth experiments) were transiently observed here and included vanillic acid and vanillin (see Table S1 in the supplemental material). With SG61-1L, vanillic acid and vanillin were observed as early as 10 min, while with SYK-6, these metabolites were observed only after 200 h (data not shown). Furthermore, GGE disappeared more quickly in SG61-1L (0.5 h) than in SYK-6 (30 h) (data not shown). Collectively, the resting-cell and growth results demonstrate that SG61-1L transforms and degrades GGE and subsequent metabolites at a significantly higher rate than SYK-6 does.

**Identification and characterization of GGE dehydrogenase candidates.** Thirteen candidate GGE dehydrogenase genes identified from the assembled SG61-1L genome were selected for expression and further characterization. These 13 genes were chosen from >100 putative dehydrogenase genes identified in the genome on the basis of their relatively high percentages of amino acid identity to those for LigD, LigO, LigL, or LigN in SYK-6 and/or proximity to other genes in the genome that may be involved in lignin degradation (Table 1). The 13 sequences selected showed 20 to 67% amino acid identity with the SYK-6 dehydrogenases and demonstrated various levels of genomic context. For

example, the SG61-1L gene for 724 was not surrounded by genes with annotated roles in lignin degradation but showed high identity with the gene for LigO (39%), while the SG61-1L gene for 3344 was adjacent to two glutathione transferase genes and other genes potentially involved in lignin degradation but showed only 17 to 22% percent identity to the four SYK-6 GGE dehydrogenase genes.

All 13 dehydrogenase genes from SG61-1L, along with the four originally characterized GGE dehydrogenase genes from SYK-6, were cloned and overexpressed in *E. coli*, and the corresponding enzymes were purified. Three of the SG61-1L enzymes were insoluble (those for 2549, 3191, and 2706) and therefore unable to be assayed, while three others from this bacterium (those for 3730, 3175, and 3726) were soluble but did not demonstrate any detectable dehydrogenase activity with the GGE substrate. The kinetic constants for the remaining seven SG61-1L enzymes and the four from SYK-6 are reported in Table 3. The enzymatic reaction was verified by LC-MS to confirm the *in vitro* transformation of GGE to MPPHV (Fig. 3).

All four SYK-6 GGE dehydrogenases were able to degrade all four GGE stereoisomers. In general, LigN and LigL displayed higher turnover rates than LigD and LigO for all four stereoisomers (Table 3). Our  $k_{cat}$  values for LigD and LigN correlate with previous data in that they demonstrate the fastest turnover of ( $\alpha$ R, $\beta$ R)-/( $\alpha$ R, $\beta$ S)-GGE and ( $\alpha$ S, $\beta$ S)-GGE, respectively; however, aspects of our experimental results do not correlate well with previous data from SYK-6. For example, according to our  $k_{cat}$  values, LigO displays the highest turnover rate for ( $\alpha$ S, $\beta$ S)-GGE and not ( $\alpha$ R, $\beta$ R)- or ( $\alpha$ R, $\beta$ S)-GGE, as reported previously (33). Additionally, the majority of the  $K_m$  and  $k_{cat}/K_m$  values for each enzyme do not correlate with the previously reported stereoisomer preferences, assuming that the preferred stereoisomer would generate a lower  $K_m$  value and a higher  $k_{cat}/K_m$  value than other stereoisomers for a given enzyme. These discrepancies can be explained by the fact that very different methods of analysis were employed in the two sets of experiments. While the previous report determined enzyme stereoselectivity through genetic knockouts (for LigD) or enzyme performance in crude cell extracts in the presence of two stereoisomers (for LigD, LigN, and LigL), all of our experiments were performed *in vitro* with purified enzymes in the presence of a single stereoisomer. Thus, differences in enzyme concentrations, for example, would have influenced the earlier results but not ours.

Two of the SG61-1L enzymes, 724 and 2550, turned over all four stereoisomers very efficiently, with  $k_{cat}$  values up to 550-fold higher than those of the SYK-6 enzymes (Table 3). SG61-1L 724 had the highest  $k_{cat}$  values for all of the stereoisomers and the highest specificity constant estimates for two stereoisomers [360 and 368  $\mu\text{M}^{-1} \text{s}^{-1}$  for ( $\alpha$ R, $\beta$ S)-GGE and ( $\alpha$ R, $\beta$ R)-GGE, respectively]. SG61-1L 2550 had significantly lower  $K_m$  values (3.6 and 0.8  $\mu\text{M}$ , respectively) for the other two stereoisomers, ( $\alpha$ S, $\beta$ R)-GGE and ( $\alpha$ S, $\beta$ S)-GGE, yielding specificity constant estimates of 12.9 and 95.1  $\mu\text{M}^{-1} \text{s}^{-1}$ , respectively. SG61-1L 724 and 2550 both showed relatively high sequence identity to the SYK-6 GGE dehydrogenases (30 to 39% and 30 to 47%, respectively). Three other SG61-1L enzymes, 3329, 2705, and 1498, also show high sequence identity with SYK-6 enzymes (28 to 31%, 34 to 42%, and 30 to 67%, respectively) but performed relatively poorly in kinetic assays. Interestingly, the two remaining enzymes, 3344 and 474, performed similarly to or better than the latter three enzymes despite

TABLE 3 Kinetic constants for short-chain dehydrogenases from SG61-1L and SYK-6 on all GGE stereoisomers

Constant and name	( $\alpha$ S, $\beta$ R)-GGE	( $\alpha$ R, $\beta$ S)-GGE	( $\alpha$ R, $\beta$ R)-GGE	( $\alpha$ S, $\beta$ S)-GGE
$K_m$ , GGE ( $\mu$ M)				
LigD	0.39 $\pm$ 0.08	15 $\pm$ 13	25 $\pm$ 10	12.2 $\pm$ 2.3
LigL	1.6 $\pm$ 0.3	39 $\pm$ 5	3.0 $\pm$ 0.5	61 $\pm$ 16
LigN	51 $\pm$ 14	15.3 $\pm$ 2.8	1.7 $\pm$ 0.3	35.0 $\pm$ 7.2
LigO	118 $\pm$ 29	1.2 $\pm$ 0.4	51 $\pm$ 12	40.3 $\pm$ 9.6
2550	3.6 $\pm$ 0.6	53 $\pm$ 9	2.2 $\pm$ 0.8	0.8 $\pm$ 0.2
1498	88 $\pm$ 15	ND <sup>a</sup>	ND	57 $\pm$ 12
2705	357 $\pm$ 47	235 $\pm$ 41	ND	354 $\pm$ 44
3329	ND	ND	49 $\pm$ 16	35 $\pm$ 10
3344	66 $\pm$ 12	202 $\pm$ 16	19.0 $\pm$ 3.0	162 $\pm$ 24
474	109 $\pm$ 18	ND	ND	163 $\pm$ 22
724	77 $\pm$ 18	2.0 $\pm$ 0.4	4.2 $\pm$ 0.8	33.7 $\pm$ 8.8
$k_{cat}$ ( $s^{-1}$ )				
LigD	4.9 $\pm$ 0.2	17.0 $\pm$ 3.7	22.7 $\pm$ 2.9	8.4 $\pm$ 0.4
LigL	83.4 $\pm$ 0.1	76.5 $\pm$ 3.8	33.9 $\pm$ 1.0	381 $\pm$ 0.6
LigN	50.6 $\pm$ 5.1	65.2 $\pm$ 3.1	25.4 $\pm$ 1.0	67.4 $\pm$ 5.6
LigO	7.0 $\pm$ 0.7	2.8 $\pm$ 0.2	3.0 $\pm$ 0.3	15.6 $\pm$ 1.5
2550	46.1 $\pm$ 2.3	117 $\pm$ 6	15.9 $\pm$ 1.5	74.2 $\pm$ 2.7
1498	3.9 $\pm$ 0.3	ND	ND	2.6 $\pm$ 0.2
2705	50.8 $\pm$ 3.0	2.8 $\pm$ 0.2	ND	66.1 $\pm$ 4.0
3329	ND	ND	0.6 $\pm$ 0.1	0.1 $\pm$ 0.01
3344	2.3 $\pm$ 0.2	2.3 $\pm$ 0.1	0.3 $\pm$ 0.01	197 $\pm$ 10
474	1.5 $\pm$ 0.1	ND	ND	12.5 $\pm$ 0.8
724	942 $\pm$ 83	701 $\pm$ 27	1534 $\pm$ 62	722 $\pm$ 66
$k_{cat}/K_m$ , GGE ( $\mu$ M <sup>-1</sup> s <sup>-1</sup> )				
LigD	12.5 $\pm$ 2.7	1.14 $\pm$ 1.06	0.92 $\pm$ 0.4	0.68 $\pm$ 0.13
LigL	53.3 $\pm$ 9.0	1.9 $\pm$ 0.3	11.3 $\pm$ 2.1	6.3 $\pm$ 1.7
LigN	1.0 $\pm$ 0.3	4.2 $\pm$ 0.8	15.1 $\pm$ 2.9	2.0 $\pm$ 0.4
LigO	0.06 $\pm$ 0.01	2.4 $\pm$ 0.8	0.06 $\pm$ 0.01	0.39 $\pm$ 0.10
2550	12.9 $\pm$ 2.4	2.2 $\pm$ 0.4	7.4 $\pm$ 2.7	95.1 $\pm$ 20
1498	0.04 $\pm$ 0.01	ND	ND	0.05 $\pm$ 0.01
2705	0.14 $\pm$ 0.02	0.012 $\pm$ 0.002	ND	0.18 $\pm$ 0.03
3329	ND	ND	0.012 $\pm$ 0.004	0.003 $\pm$ 0.001
3344	0.03 $\pm$ 0.01	0.011 $\pm$ 0.001	0.015 $\pm$ 0.003	1.2 $\pm$ 0.2
474	0.013 $\pm$ 0.002	ND	ND	0.08 $\pm$ 0.01
724	12.4 $\pm$ 3.1	360 $\pm$ 74	368 $\pm$ 69	21.4 $\pm$ 6.0

<sup>a</sup> ND, no detectable activity.

their low levels of sequence identity to the SYK-6 enzymes (17 to 22% and 15 to 19%, respectively) (Table 1). Aside from SG61-1L 3344 and 3329, which used the cofactor NADP<sup>+</sup>, all of the other SG61-1L enzymes functioned with the cofactor NAD<sup>+</sup>. The four SYK-6 enzymes also preferred the cofactor NAD<sup>+</sup>, as determined in previous experiments (33).

There was no obvious relationship between the kinetic parameters of any individual SG61-1L enzyme for the different stereoisomers and the relative degradation rates of those isomers in the growth experiments. This is perhaps unsurprising, given that (i) several of the enzymes have relatively good kinetics for one or more of the isomers, (ii) we do not know the relative importance of  $k_{cat}$  and  $K_m$  to degradation rates under the conditions of the growth experiment, (iii) we do not know the relative abundances of the enzymes *in vivo*, and (iv) there may be other dehydrogenases in the organism that are uncharacterized but also contribute to GGE oxidation.

**Phylogenetic relationships between dehydrogenases from related organisms.** A phylogenetic tree was constructed in an attempt to articulate relationships among sequence, function, and

stereoselectivity among the dehydrogenases characterized in this study (Fig. 4). For contextual purposes, 136 additional sequences showing  $\geq 20\%$  amino acid identity to at least one of the characterized SYK-6 and SG61-1L dehydrogenases were included in the phylogeny. These sequences were from three bacteria, one that was tested (along with SYK-6 and SG61-1L) and unable to degrade GGE (*P. putida* KT2440) and two that were not known to degrade GGE (*N. aromaticivorans* DSM12444 and *S. chlorophenicum* L-1). Notably, *N. aromaticivorans* DSM12444 may have the ability to degrade GGE, given that it encodes active MPPHV  $\beta$ -etherase GSTs (37), as well as several putative C-alpha-dehydrogenases with relatively high sequence identity (37 to 76%) to one or more of the SYK-6 enzymes. Nineteen sequences from other bacteria that produce enzymes with experimentally verified activities were also included in the tree; all of these sequences showed  $\geq 20\%$  amino acid identity to characterized SYK-6 and SG61-1L dehydrogenases, as described in Materials and Methods. As shown in Fig. 4, the 4 SYK-6 GGE dehydrogenases and 7 of the 13 SG61-1L dehydrogenases chosen in this study cluster together in the same clade. Moreover, this clade does not include any amino acid se-

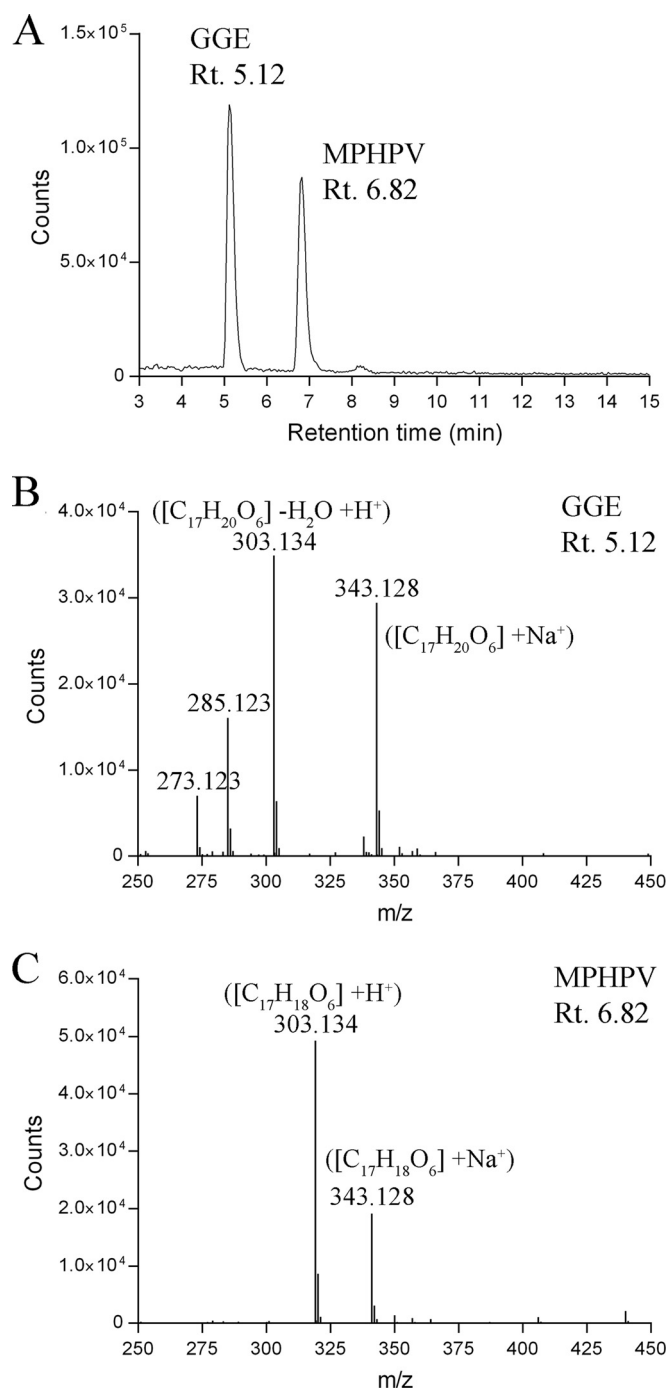


**FIG 3** Enzymatic conversion of GGE to MPHPV. (A) LC-MS chromatogram of an enzymatic reaction with the SG-61-1L 724 enzyme and the GGE substrate showing conversion of GGE to MPHPV. (B) The mass spectrum for the peak at a retention time of 5.12 min (GGE). (C) The mass spectrum for the peak at a retention time of 6.82 min (MPHPV).

quences from the non-GGE-degrading bacterium *P. putida* but does include five amino acid sequences from *N. aromaticivorans* and one from *S. chlorophenolicum*. With the exception of SG61-1L 2706 and 2549, which were completely insoluble, all of the remaining SG61-1L dehydrogenases in this clade displayed activity on the GGE stereoisomers, and this clade was therefore named the

“GGE-dehydrogenase clade” (Fig. 4). SG61-1L 3344 and 474 lay outside the GGE-dehydrogenase clade, despite the fact that they displayed measurable activities on two or more GGE stereoisomers (Table 3; Fig. 4).

## DISCUSSION

Here we report the isolation of SG61-1L, a bacterium that is able to degrade the GGE model lignin dimer at a much higher rate than the previously characterized GGE-degrading bacterium SYK-6. In order to understand the molecular basis for its activity and investigate the biotechnological potential of the enzymes involved, we have proceeded to characterize a suite of its dehydrogenases that are prime candidates for the first step in  $\beta$ -aryl ether degradation, the  $NAD(P)^+$ -dependent oxidation of GGE to MPHPV.

Our analyses suggest that the four SYK-6 enzymes are kinetically inferior to two of the SG61-1L enzymes, 724 and 2550, as catalysts for all four stereoisomers. This result may, in part, explain the higher rate of GGE transformation observed in SG61-1L. C-alpha-dehydrogenases that were previously purified from *Pseudomonas* spp. have  $K_m$  values for GGE (represented by a mixture of stereoisomers) as low as 11 to 12  $\mu M$  ( $k_{cat}$  values were not reported) (28, 32), but the genes encoding these proteins were not identified; interestingly, the monomeric molar mass of the C-alpha-dehydrogenase from *Pseudomonas* sp. strain GU5 was estimated to be approximately 52,000 kDa (28), which is quite different from the average monomeric molar mass range of all of the characterized proteins in this work (approximately 30,000 kDa), suggesting that perhaps another, as-yet-unidentified, type of C-alpha-dehydrogenase in this organism can oxidize GGE.

Most of the enzymes with GGE dehydrogenase activity characterized herein fall into a single clade, and it is likely that this clade in general is a good predictor of GGE dehydrogenase activity. It is also apparent that the sequences of GGE dehydrogenases in this clade have diverged significantly from other functionally annotated dehydrogenases (Fig. 4). Three additional uncharacterized SYK-6 genes are also present in the GGE dehydrogenase clade, but it seems unlikely that they play a larger role in GGE oxidation than those already characterized. This notion is based on a previous experiment with a mutant SYK-6 bacterium containing knockouts of three GGE dehydrogenase genes (those for LigD, LigN, and LigL) that result in nearly complete loss of the ability to oxidize GGE compared to that of the wild type (33).

Under the selection pressures imposed on bacteria in an environment that is rich in lignin-derived substructures, it is possible that dehydrogenases outside the GGE dehydrogenase clade and native to other metabolic pathways (such as 3344 and 474) have evolved some ability to contribute to GGE oxidation. For example, 3344 and 3730 localize to a larger clade of the phylogenetic tree that contains a functionally verified levodione reductase from *Corynebacterium aquaticum* M-13; 3344 and 3730 show 38 and 43% amino acid identity to this levodione reductase, respectively, indicating that 3344 may have evolved from a levodione reductase (perhaps 3730) encoded in the SG61-1L genome. This idea that biological degradation occurs through multiple unrelated dehydrogenases native to different pathways is reminiscent of a recent report on the oxidation of dehydrodiconiferyl aldehyde in SYK-6, which is proposed to occur through the action of several aldehyde dehydrogenases (49). SYK-6 and SG61-1L were both isolated from pulp and paper mill waste sites (50), but unlike SYK-6, SG61-1L was specifically selected through rounds of enrichment

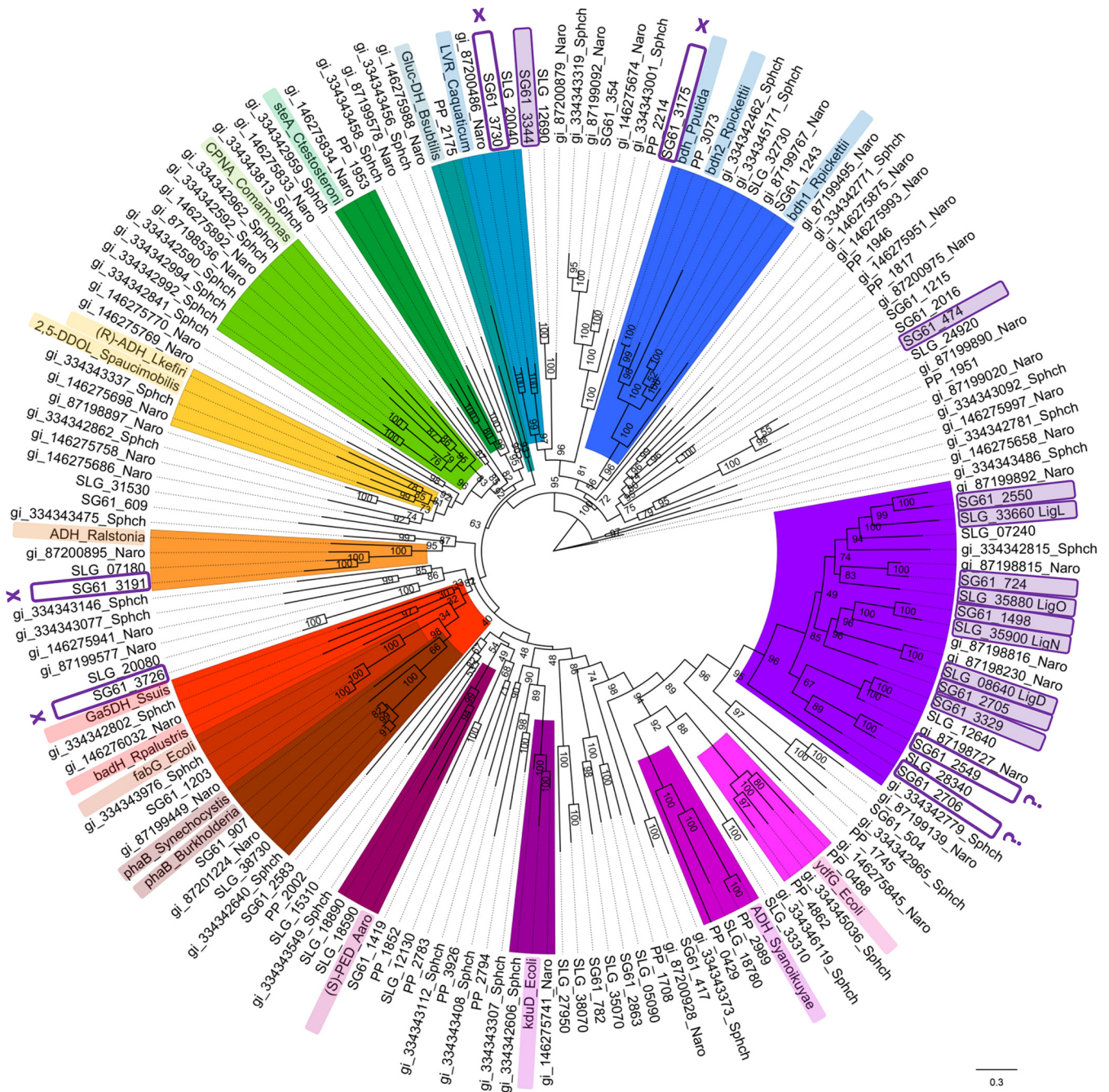


**FIG 4** Phylogenetic tree of GGE dehydrogenase proteins and their closest relatives from five different organisms, including SG61-1L (SG61), SKY-6 (SLG), *P. putida* KT2440 (PP), *N. aromaticivorans* DSM12444 (Naro), and *S. chloropheniculum* L-1 (Sphch). Also included in the alignment were amino acid sequences deduced from genes from a variety of bacteria whose annotations have been experimentally verified (names are highlighted in various colors, and abbreviations are defined below; for the references, see Table S2 in the supplemental material). The clades most closely related to each verified amino acid sequence are colored in the same shade. The purple clade represents the GGE dehydrogenase clade identified in this work. The names of the SG61-1L and SYK-6 enzymes characterized here are shaded and outlined if they exhibited GGE dehydrogenase activity and are otherwise outlined (insoluble enzymes are indicated by a question mark, while enzymes that displayed no activity are indicated by the letter X). See Table S2 in the supplemental material for the accession numbers of all of the genes (corresponding to the representative amino acid sequences) in the tree that are not represented by gene identification (gi) numbers (Naro and Sphch) or locus IDs (SLG and PP). Abbreviations: ydfG\_Ecoli, 3-hydroxy acid dehydrogenase from *E. coli* (light pink); ADH\_Syanoikuyae, “bulky-bulky” ketone dehydrogenase from *Sphingobium yanoikuyae* DSM6900 (magenta); kduD\_Ecoli, 2-dehydro-3-deoxy-D-gluconate dehydrogenase from *E. coli* (fuchsia); (S)-PED\_Aaro, (S)-1-phenylethanol dehydrogenase from *Aromatoleum aromaticum* EbN1 (plum); phaB\_Burkholderia, acetoacetyl coenzyme A reductase from *Burkholderia* sp. strain RPE75 (brown); phaB\_Synechocystis, acetoacetyl coenzyme A reductase from *Synechocystis* sp. strain PCC6803 (brown); fabG\_Ecoli,  $\beta$ -ketoacyl-[acyl carrier protein] reductase from *E. coli* (maroon); badH\_Rpalustris, 2-hydroxycyclohexanecarboxyl-coenzyme A dehydrogenase from *Rhodospseudomonas palustris* CGA009 (red); Ga5DH\_Ssuis, gluconate 5-dehydrogenase from *Streptococcus suis* (red); ADH\_Ralstonia, “bulky-bulky” alcohol dehydrogenase from *Ralstonia* sp. strain DSM6428 (orange); 2,5-DDOL\_Spaucimobilis, 2,5-dichloro-2,5-cyclohexadiene-1,4-diol dehydrogenase from *Sphingomonas paucimobilis* UT26 (yellow); (R)-ADH\_Lkefiri, (R)-specific alcohol dehydrogenase from *Lactobacillus kefirii* (yellow); CPNA\_Comamonas, cyclopentanone dehydrogenase from *Comamonas* sp. strain NCIMB 9872 (light green); steA\_Ctestosteroni,  $7\alpha, 12\alpha$ -dihydroxyandrosta-1,4-diene-3,17-dione dehydrogenase from *Comamonas testosteroni* TA441 (dark green); Gluc-DH\_Bsubtilis, glucose 1-dehydrogenase from *Bacillus subtilis* (turquoise); LVR\_Caquaticum, levodione reductase from *Corynebacterium aquaticum* M-13 (light blue); bdh\_Pputida, 3-hydroxybutyrate dehydrogenase from *P. putida* ZIMET 10947 (dark blue); bdh1\_ and bdh2\_Rpickettii, 3-hydroxybutyrate dehydrogenase from *Ralstonia pickettii* T1 (dark blue).

culturing for the ability to utilize GGE as a sole carbon source. This difference is perhaps reflected in the poorer kinetic parameters of the SYK-6 GGE dehydrogenases than the two highest-performing SG61-1L GGE dehydrogenases.

There is no obvious correlation between phylogeny and stereoselectivity within the GGE dehydrogenase clade. For example, 1498 from SG61-1L and LigN from SYK-6 show the highest sequence identity (67%) of any pair in the GGE dehydrogenase clade, yet 1498 was able to oxidize only the ( $\alpha$ S, $\beta$ R)- and ( $\alpha$ S, $\beta$ S)-GGE stereoisomers while LigN could oxidize all four. Similarly, 2550 from SG61-1L and LigL from SYK-6 also cluster together in this clade (Fig. 4) and were both able to oxidize all four GGE stereoisomers, but each enzyme displayed a different pattern of stereospecificity (Table 3). We suspect that empirical structural data will be necessary to identify the sequence motifs guiding stereoselectivity preferences among these GGE dehydrogenases.

To the best of our knowledge, SG61-1L is one of the fastest known bacterial degraders of a lignin substructure; previously reported rates of bacterial degradation for model lignin dimers are quite low (38, 39), albeit various conditions were used and the results may therefore not be directly comparable. We report here that SG61-1L can degrade GGE much faster than SYK-6 can under the same experimental conditions and that in SYK-6, transformation of MPHPV to  $\alpha$ -glutathionyl- $\beta$ -HPV (GS-HPV) appears to be a rate-limiting step.

Following GGE oxidation to MPHPV, the enzymes that perform the next two reactions (the  $\beta$ -etherase reaction to generate GS-HPV, followed by glutathione removal to generate achiral HPV) are GSTs. They have been identified as LigF-LigE-LigP and LigG, respectively, in SYK-6, and homologs have been functionally verified in closely related sphingomonads (34–37), including *N. aromaticivorans* DSM12444, which also contains genes present in the GGE dehydrogenase clade. There are several uncharacterized GSTs in the SG61-1L genome, two of which have the highest sequence identity to LigP (63 to 79%) and five of which have the highest sequence identity to LigF (34 to 59%). Curiously, none of the SG61-1L-encoded GSTs have high sequence identity to LigG (<17%). Thus, there are several candidates in SG61-1L for the first GST step, but the second apparently involves an enzyme not closely related to LigG. Given that the LigG reaction in SYK-6 is specific to only one of the two GS-HPV stereoisomers (36), it has also been suggested that there is at least one other, as-yet-uncharacterized, GST with activity for the other GS-HPV stereoisomer in SYK-6. Future work will involve the characterization of these later steps in the pathway in order to articulate mechanisms by which SG61-1L proceeds through GGE degradation at a relatively high rate.

There is an emerging interest in the development of lignin-degrading enzymes for industrial purposes, especially for integration into processes generating replacements for petroleum-based commodities. Selective depolymerization of lignin or lignin components could generate high-value, complex aromatics, including catechols, resorcinols, keto acids, and polyhydroxy aromatics (2, 51). Vanillin, for example, has been produced from lignocelluloses in a *Rhodococcus jostii* RHA-1 mutant (52). Vanillin also has potential to be produced on a large scale via the biodegradation of lignin substructures (such as  $\beta$ -aryl ether-linked lignin dimers) by engineered versions of bacteria such as SG61-1L and SYK-6 or by free enzymes driving the relevant reactions derived from them (5, 53). Thus far, we have characterized a group of dehydrogenases

from SG61-1L that are involved in the first step of a lignin degradation pathway and could be used to produce a high-value chemical such as vanillin. The priorities of a high  $k_{cat}$  versus a low  $K_m$  and broad versus narrow stereoselectivity for a given enzyme will vary, depending on the process, but the suite of dehydrogenases from SG61-1L that we have characterized provides a wide range of options across these criteria. Any further protein engineering required to make promising enzymes more fit for a purpose can also now be guided by our findings on the phylogenetic distribution of GGE dehydrogenase activity. SG61-1L is also a very promising source of catalysts for downstream steps in the GGE degradation pathway, particularly the  $\beta$ -etherase step, which results in cleavage of the highly stable aryl-aryl ether bond of MPHPV to produce GS-HPV.

## ACKNOWLEDGMENTS

We thank Shojiro Hishiyama (Forestry and Forest Products Research Institute, Tsukuba, Ibaraki, Japan) and Eiji Masai (Department of Bioengineering, Nagaoka University of Technology, Nagaoka, Niigata, Japan) for providing the four separate GGE stereoisomers and Lars Jermiin (CSIRO) for his assistance with the generation of protein sequence alignments and all of the accompanying processes involved in phylogenetic tree construction. We also thank Chris Coppin (CSIRO) for his unconditional support throughout the study.

N.D. was supported by the CSIRO Office of the Chief Executive (OCE) Postdoctoral Fellowship scheme.

## REFERENCES

- Ragauskas AJ, Beckham GT, Biddy MJ, Chandra R, Chen F, Davis MF, Davison BH, Dixon RA, Gilna P, Keller M, Langan P, Naskar AK, Saddler JN, Tschaplinski TJ, Tuskan GA, Wyman CE. 2014. Lignin valorization: improving lignin processing in the biorefinery. *Science* 344:1246843. <http://dx.doi.org/10.1126/science.1246843>.
- Holladay JE, Bozell JJ, White JF, Johnson D. 2007. Top value-added chemicals from biomass. Volume II—results of screening for potential candidates from biorefinery lignin. Pacific Northwest National Laboratory, Richland, WA. [http://www.pnl.gov/main/publications/external/technical\\_reports/PNNL-16983.pdf](http://www.pnl.gov/main/publications/external/technical_reports/PNNL-16983.pdf).
- Weng JK, Chapple C. 2010. The origin and evolution of lignin biosynthesis. *New Phytol* 187:273–285. <http://dx.doi.org/10.1111/j.1469-8137.2010.03327.x>.
- Bugg TDH, Ahmad M, Hardiman EM, Rahmanpour R. 2011. Pathways for degradation of lignin in bacteria and fungi. *Nat Prod Rep* 28:1883–1896. <http://dx.doi.org/10.1039/c1np00042j>.
- Masai E, Katayama Y, Fukuda M. 2007. Genetic and biochemical investigations on bacterial catabolic pathways for lignin-derived aromatic compounds. *Biosci Biotechnol Biochem* 71:1–15. <http://dx.doi.org/10.1271/bbb.60437>.
- Leonowicz A, Cho NS, Luterek J, Wilkolazka A, Wojtas-Wasilewska M, Matuszewska A, Hofrichter M, Wesenberg D, Rogalski J. 2001. Fungal laccase: properties and activity on lignin. *J Basic Microbiol* 41:185–227. [http://dx.doi.org/10.1002/1521-4028\(200107\)41:3/4<185::AID-JOBM185>3.0.CO;2-T](http://dx.doi.org/10.1002/1521-4028(200107)41:3/4<185::AID-JOBM185>3.0.CO;2-T).
- Martínez AT, Speranza M, Ruiz-Duenas FJ, Ferreira P, Camarero S, Guillen F, Martínez MJ, Gutiérrez A, del Río JC. 2005. Biodegradation of lignocelluloses: microbial, chemical, and enzymatic aspects of the fungal attack of lignin. *Int Microbiol* 8:195–204.
- Ramachandra M, Crawford DL, Hertel G. 1988. Characterization of an extracellular lignin peroxidase of the lignocellulolytic actinomycete *Streptomyces viridosporus*. *Appl Environ Microbiol* 54:3057–3063.
- Brown ME, Barros T, Chang MCY. 2012. Identification and characterization of a multifunctional dye peroxidase from a lignin-reactive bacterium. *ACS Chem Biol* 7:2074–2081. <http://dx.doi.org/10.1021/cb300383y>.
- Majumdar S, Lukk T, Solbiati JO, Bauer S, Nair SK, Cronan JE, Gerlt JA. 2014. Roles of small laccases from *Streptomyces* in lignin degradation. *Biochemistry* 53:4047–4058. <http://dx.doi.org/10.1021/bi500285t>.
- Min K, Gong G, Woo HM, Kim Y, Um Y. 2015. A dye-decolorizing peroxidase from *Bacillus subtilis* exhibiting substrate-dependent opti-

- mum temperature for dyes and  $\beta$ -ether lignin dimer. *Sci Rep* 5:8245. <http://dx.doi.org/10.1038/srep08245>.
12. Taylor CR, Hardiman EM, Ahmad M, Sainsbury PD, Norris PR, Bugg TDH. 2012. Isolation of bacterial strains able to metabolize lignin from screening of environmental samples. *J Appl Microbiol* 113:521–530. <http://dx.doi.org/10.1111/j.1365-2672.2012.05352.x>.
  13. Ahmad M, Roberts JN, Hardiman EM, Singh R, Eltis LD, Bugg TDH. 2011. Identification of DypB from *Rhodococcus jostii* RHA1 as a lignin peroxidase. *Biochemistry* 50:5096–5107. <http://dx.doi.org/10.1021/bi101892z>.
  14. Bugg TDH, Ahmad M, Hardiman EM, Singh R. 2011. The emerging role for bacteria in lignin degradation and bio-product formation. *Curr Opin Biotechnol* 22:394–400. <http://dx.doi.org/10.1016/j.copbio.2010.10.009>.
  15. Brown ME, Chang MCY. 2014. Exploring bacterial lignin degradation. *Curr Opin Chem Biol* 19:1–7. <http://dx.doi.org/10.1016/j.cbpa.2013.11.015>.
  16. Wang YX, Liu Q, Yan L, Gao YM, Wang YJ, Wang WD. 2013. A novel lignin degradation bacterial consortium for efficient pulping. *Bioresour Technol* 139:113–119. <http://dx.doi.org/10.1016/j.biortech.2013.04.033>.
  17. Salvachua D, Karp EM, Nimlos CT, Vardon DR, Beckham GT. 3 June 2015. Towards lignin consolidated bioprocessing: simultaneous lignin depolymerization and product generation by bacteria. *Green Chem* <http://dx.doi.org/10.1039/C5GC01165E>.
  18. Strachan CR, Singh R, VanInsberghe D, Ievdokymenko K, Budwill K, Mohn WW, Eltis LD, Hallam SJ. 2014. Metagenomic scaffolds enable combinatorial lignin transformation. *Proc Natl Acad Sci U S A* 111:10143–10148. <http://dx.doi.org/10.1073/pnas.1401631111>.
  19. Lu LH, Zeng GM, Fan CZ, Zhang JC, Chen AW, Chen M, Jiang M, Yuan YJ, Wu HP, Lai MY, He YB. 2014. Diversity of two-domain laccase-like multicopper oxidase genes in *Streptomyces* spp.: identification of genes potentially involved in extracellular activities and lignocellulose degradation during composting of agricultural waste. *Appl Environ Microbiol* 80:3305–3314. <http://dx.doi.org/10.1128/AEM.00223-14>.
  20. Chai LY, Chen YH, Tang CJ, Yang ZH, Zheng Y, Shi Y. 2014. Depolymerization and decolorization of kraft lignin by bacterium *Comamonas* sp. B-9. *Appl Microbiol Biotechnol* 98:1907–1912. <http://dx.doi.org/10.1007/s00253-013-5166-5>.
  21. Shi Y, Chai LY, Tang CJ, Yang ZH, Zheng Y, Chen YH, Jing QX. 2013. Biochemical investigation of kraft lignin degradation by *Pandora* sp. B-6 isolated from bamboo slips. *Bioprocess Biosyst Eng* 36:1957–1965. <http://dx.doi.org/10.1007/s00449-013-0972-9>.
  22. Shi Y, Chai LY, Tang CJ, Yang ZH, Zhang H, Chen RH, Chen YH, Zheng Y. 2013. Characterization and genomic analysis of kraft lignin biodegradation by the beta-proteobacterium *Cupriavidus basilensis* B-8. *Biotechnol Biofuels* 6:1. <http://dx.doi.org/10.1186/1754-6834-6-1>.
  23. Singh R, Grigg JC, Qin W, Kadla JF, Murphy MEP, Eltis LD. 2013. Improved manganese-oxidizing activity of DypB, a peroxidase from a lignolytic bacterium. *ACS Chem Biol* 8:700–706. <http://dx.doi.org/10.1021/cb300608x>.
  24. Vicuña R. 1988. Bacterial degradation of lignin. *Enzyme Microb Technol* 10:646–655. [http://dx.doi.org/10.1016/0141-0229\(88\)90055-5](http://dx.doi.org/10.1016/0141-0229(88)90055-5).
  25. Zimmermann W. 1990. Degradation of lignin by bacteria. *J Biotechnol* 13:119–130. [http://dx.doi.org/10.1016/0168-1656\(90\)90098-V](http://dx.doi.org/10.1016/0168-1656(90)90098-V).
  26. Seelenfreund D, Ruttimann C, Vicuña R. 1986. Metabolism of lignin model compounds by *Streptomyces viridosporus* T7a. *Arch Biol Med Exp* 19:R253–R253.
  27. Samejima M, Abe S, Saburi Y, Yoshimoto T. 1988. Metabolism of lignin model compounds with  $\beta$ -aryl ether linkage by *Pseudomonas* sp. TMY1009 and its mutants. *Cellul Chem Technol* 22:279–286.
  28. Pelmont J, Barrelle M, Hauteville M, Gamba D, Romdhane M, Dardas A, Beguin C. 1985. A new bacterial dehydrogenase oxidizing the lignin model compound guaiacylglycerol  $\beta$ -O-4-guaiacyl ether. *Biochimie* 67:973–986. [http://dx.doi.org/10.1016/S0300-9084\(85\)80292-3](http://dx.doi.org/10.1016/S0300-9084(85)80292-3).
  29. Vasudevan N, Mahadevan A. 1991. Degradation of lignin and lignin derivatives by *Acinetobacter* sp. *J Appl Bacteriol* 70:169–176. <http://dx.doi.org/10.1111/j.1365-2672.1991.tb04444.x>.
  30. Vasudevan N, Mahadevan A. 1992. Degradation of nonphenolic  $\beta$ -O-4 lignin substructure model compounds by *Acinetobacter* sp. *Res Microbiol* 143:333–339. [http://dx.doi.org/10.1016/0923-2508\(92\)90025-J](http://dx.doi.org/10.1016/0923-2508(92)90025-J).
  31. Vicuña R, Gonzalez B, Mozuch MD, Kirk TK. 1987. Metabolism of lignin model compounds of the arylglycerol- $\beta$ -aryl ether type by *Pseudomonas acidovorans* D(3). *Appl Environ Microbiol* 53:2605–2609.
  32. Habu N, Samejima M, Saburi Y, Yoshimoto T. 1988. Purification and some properties of 2 C- $\alpha$ -dehydrogenases oxidizing dimeric lignin model compounds from *Pseudomonas* sp. TMY1009. *Agric Biol Chem* 52:3073–3079. <http://dx.doi.org/10.1271/abb1961.52.3073>.
  33. Sato Y, Moriuchi H, Hishiyama S, Otsuka Y, Oshima K, Kasai D, Nakamura M, Ohara S, Katayama Y, Fukuda M, Masai E. 2009. Identification of three alcohol dehydrogenase genes involved in the stereospecific catabolism of arylglycerol- $\beta$ -aryl ether by *Sphingobium* sp. strain SYK-6. *Appl Environ Microbiol* 75:5195–5201. <http://dx.doi.org/10.1128/AEM.00880-09>.
  34. Masai E, Ichimura A, Sato Y, Miyauchi K, Katayama Y, Fukuda M. 2003. Roles of the enantioselective glutathione S-transferases in cleavage of  $\beta$ -aryl ether. *J Bacteriol* 185:1768–1775. <http://dx.doi.org/10.1128/JB.185.6.1768-1775.2003>.
  35. Tanamura K, Abe T, Kamimura N, Kasai D, Hishiyama S, Otsuka Y, Nakamura M, Kajita S, Katayama Y, Fukuda M, Masai E. 2011. Characterization of the third glutathione S-transferase gene involved in enantioselective cleavage of the  $\beta$ -aryl ether by *Sphingobium* sp. strain SYK-6. *Biosci Biotechnol Biochem* 75:2404–2407. <http://dx.doi.org/10.1271/bbb.110525>.
  36. Gall DL, Kim H, Lu FC, Donohue TJ, Noguera DR, Ralph J. 2014. Stereochemical features of glutathione-dependent enzymes in the *Sphingobium* sp. strain SYK-6  $\beta$ -aryl etherase pathway. *J Biol Chem* 289:8656–8667. <http://dx.doi.org/10.1074/jbc.M113.536250>.
  37. Gall DL, Ralph J, Donohue TJ, Noguera DR. 2014. A group of sequence-related sphingomonad enzymes catalyzes cleavage of  $\beta$ -aryl ether linkages in lignin  $\beta$ -guaiacyl and  $\beta$ -syringyl ether dimers. *Environ Sci Technol* 48:12454–12463. <http://dx.doi.org/10.1021/es503886d>.
  38. Huang XF, Santhanam N, Badri DV, Hunter WJ, Manter DK, Decker SR, Vivanco JM, Reardon KF. 2013. Isolation and characterization of lignin-degrading bacteria from rainforest soils. *Biotechnol Bioeng* 110:1616–1626. <http://dx.doi.org/10.1002/bit.24833>.
  39. Kuhnigk T, König H. 1997. Degradation of dimeric lignin model compounds by aerobic bacteria isolated from the hindgut of xylophagous termites. *J Basic Microbiol* 37:205–211. <http://dx.doi.org/10.1002/jobm.3620370309>.
  40. Hishiyama S, Otsuka Y, Nakamura M, Ohara S, Kajita S, Masai E, Katayama Y. 2012. Convenient synthesis of chiral lignin model compounds via optical resolution: four stereoisomers of guaiacylglycerol- $\beta$ -guaiacyl ether and both enantiomers of 3-hydroxy-1-(4-hydroxy-3-methoxyphenyl)-2-(2-methoxyphenoxy)-propan-1-one (erone). *Tetrahedron Lett* 53:842–845. <http://dx.doi.org/10.1016/j.tetlet.2011.12.016>.
  41. Masai E, Katayama Y, Nishikawa S, Yamasaki M, Morohoshi N, Haraguchi T. 1989. Detection and localization of a new enzyme catalyzing the  $\beta$ -aryl ether cleavage in the soil bacterium (*Pseudomonas paucimobilis* SYK-6). *FEBS Lett* 249:348–352. [http://dx.doi.org/10.1016/0014-5793\(89\)80656-8](http://dx.doi.org/10.1016/0014-5793(89)80656-8).
  42. Bankevich A, Nurk S, Antipov D, Gurevich AA, Dvorkin M, Kulikov AS, Lesin VM, Nikolenko SI, Pham S, Pribelski AD, Pyshtkin AV, Sirotkin AV, Vyahhi N, Tesler G, Alekseyev MA, Pevzner PA. 2012. SPAdes: a new genome assembly algorithm and its applications to single-cell sequencing. *J Comput Biol* 19:455–477. <http://dx.doi.org/10.1089/cmb.2012.0021>.
  43. Katoh K, Toh H. 2010. Parallelization of the MAFFT multiple sequence alignment program. *Bioinformatics* 26:1899–1900. <http://dx.doi.org/10.1093/bioinformatics/btq224>.
  44. Nguyen LT, Schmidt HA, von Haeseler A, Minh BQ. 2015. IQ-TREE: a fast and effective stochastic algorithm for estimating maximum-likelihood phylogenies. *Mol Biol Evol* 32:268–274. <http://dx.doi.org/10.1093/molbev/msu300>.
  45. Minh BQ, Nguyen MAT, von Haeseler A. 2013. Ultrafast approximation for phylogenetic bootstrap. *Mol Biol Evol* 30:1188–1195. <http://dx.doi.org/10.1093/molbev/mst024>.
  46. Barrasa JM, Blanco MN, Esteve-Raventos F, Altes A, Checa J, Martínez AT, Ruiz-Duenas FJ. 2014. Wood and humus decay strategies by white-rot basidiomycetes correlate with two different dye decolorization and enzyme secretion patterns on agar plates. *Fungal Genet Biol* 72:106–114. <http://dx.doi.org/10.1016/j.fgb.2014.03.007>.
  47. Archibald FS. 1992. A new assay for lignin-type peroxidases employing the dye azure B. *Appl Environ Microbiol* 58:3110–3116.
  48. Camarero S, Ibarra D, Martínez MJ, Martínez AT. 2005. Lignin-derived compounds as efficient laccase mediators for decolorization of different types of recalcitrant dyes. *Appl Environ Microbiol* 71:1775–1784. <http://dx.doi.org/10.1128/AEM.71.4.1775-1784.2005>.

49. Takahashi K, Kamimura N, Hishiyama S, Hara H, Kasai D, Katayama Y, Fukuda M, Kajita S, Masai E. 2014. Characterization of the catabolic pathway for a phenylcoumaran-type lignin-derived biaryl in *Sphingobium* sp. strain SYK-6. *Biodegradation* 25:735–745. <http://dx.doi.org/10.1007/s10532-014-9695-0>.
50. Katayama Y, Nishikawa S, Nakamura M, Morohoshi N, Haraguchi T, Yano K, Yamasaki M. 1987. Cloning and expression of *Pseudomonas paucimobilis* SYK-6 genes involved in the degradation of vanillate and protocatechuate in *P. putida*. *Mokuzai Gakkaishi* 33:77–79.
51. Varanasi P, Singh P, Auer M, Adams PD, Simmons BA, Singh S. 2013. Survey of renewable chemicals produced from lignocellulosic biomass during ionic liquid pretreatment. *Biotechnol Biofuels* 6:14. <http://dx.doi.org/10.1186/1754-6834-6-14>.
52. Sainsbury PD, Hardiman EM, Ahmad M, Otani H, Seghezzi N, Eltis LD, Bugg TDH. 2013. Breaking down lignin to high-value chemicals: the conversion of lignocellulose to vanillin in a gene deletion mutant of *Rhodococcus jostii* RHA1. *ACS Chem Biol* 8:2151–2156. <http://dx.doi.org/10.1021/cb400505a>.
53. Kunjapur AM, Tarasova Y, Prather KLJ. 2014. Synthesis and accumulation of aromatic aldehydes in an engineered strain of *Escherichia coli*. *J Am Chem Soc* 136:11644–11654. <http://dx.doi.org/10.1021/ja506664a>.
54. Abe T, Masai E, Miyauchi K, Katayama Y, Fukuda M. 2005. A tetrahydrofolate-dependent *O*-demethylase, LigM, is crucial for catabolism of vanillate and syringate in *Sphingomonas paucimobilis* SYK-6. *J Bacteriol* 187:2030–2037. <http://dx.doi.org/10.1128/JB.187.6.2030-2037.2005>.
55. Misof B, Liu SL, Meusemann K, Peters RS, Donath A, Mayer C, Frandsen PB, Ware J, Flouri T, Beutel RG, Niehuis O, Petersen M, Izquierdo-Carrasco F, Wappler T, Rust J, Aberer AJ, Aspöck U, Aspöck H, Bartel D, Blanke A, Berger S, Böhm A, Buckley TR, Calcott B, Chen JQ, Friedrich F, Fukui M, Fujita M, Greve C, Grobe P, Gu SC, Huang Y, Jermiin LS, Kawahara AY, Krogmann L, Kubiak M, Lanfear R, Letsch H, Li YY, Li ZY, Li JG, Lu HR, Machida R, Mashimo Y, Kapli P, McKenna DD, Meng GL, Nakagaki Y, Navarrete-Heredia JL, Ott M, et al. 2014. Phylogenomics resolves the timing and pattern of insect evolution. *Science* 346:763–767. <http://dx.doi.org/10.1126/science.1257570>.